

Simulation of ion implantation and annealing for Si-based blocked-impurity-band detectors

Bingbing Wang

The 50th Institute, China Electronics
Technology Group Co., Shanghai, China
Shanghai Institute of Microsystem and
Information Technology, Shanghai, China
Email: wbb0308201@163.com

Yulu Chen

The 50th Institute, China Electronics
Technology Group Co., Shanghai, China
Email: yukiyulc@163.com

Haoxing Zhang

The 50th Institute, China Electronics
Technology Group Co., Shanghai, China
Email: 13022125120@163.com

Ming Pan

The 50th Institute, China Electronics
Technology Group Co., Shanghai, China
Email: 13022125120@163.com

Xiaodong Wang

The 50th Institute, China Electronics
Technology Group Co., Shanghai, China
Email: wxd06296@163.com

Juncheng Cao*

Shanghai Institute of Microsystem and
Information Technology, Shanghai, China
University of Chinese Academy of Sciences,
Chinese Academy of Sciences,
Beijing, China
Email: jccao@mail.sim.ac.cn

Abstract—The constructed structural model and the fabrication process of Si-based blocked-impurity-band (BIB) detector were proposed. To optimize the fabrication processes of Si-based BIB detector, the numerical simulation of P ion implantation and rapid thermal annealing were investigated by numerical simulation. Various implantation conditions were analyzed to meet the requirements of contact region. Moreover, the effects of rapid thermal annealing with different temperatures and time were discussed. Finally, the implantation energy of 10 keV and dose of $1 \times 10^{14} \text{ cm}^{-2}$ were adopted. The annealing temperature 900°C and holding time 10s were used. It is demonstrated that the BIB detector we fabricated with the parameters above have excellent performances.

Keywords—numerical simulation, Si-based blocked-impurity-band detector, ion implantation, rapid thermal annealing

I. INTRODUCTION

The Si-based BIB detector possesses excellent performances such as high sensitivity, large quantum efficiency, low dark current and so on [1]. Compared with the InSb detector and HgCdTe one [2], the Si-based BIB detector exhibits wider response spectral range, which covers the spectral range from infrared (IR) to terahertz (THz) region. The performance of the Si-based BIB detector is proved to be closely related to dopant, device structure, host material, and fabrication process. Extensive efforts have been made to improve the performance of BIB detector.

Stephan M. Birkmann et al. reported that the Si:As BIB detector for the European Space Agency (ESA) in the framework of the future Darwin mission could response a wide spectral range from 4 to $28 \mu\text{m}$ [3]. The epitaxial Si:Sb BIB detectors prepared by James E. Huffman et al. are sensitive to radiations between 2.5 and $40 \mu\text{m}$, and the peak responsivity

could reach as high as 36A/W [4]. Compared with traditional front-illuminated BIB detector, the back illuminated blocked-impurity-band (BIBIB) detector and Ion-implantation Blocked-Impurity-Band detector (IBIB) one were explored by S.B.Stetson and Jeffrey W. Beeman, respectively [5, 6]. To further extend the response spectrum range, different host materials were employed, such as Si, Ge and GaAs. Dan M. Watson's result shows that the shallow dopant energy level in Ge-based BIB detector will lead to the spectral response from 40 to $200 \mu\text{m}$ [7]. According to the results by Wang et al., the spectral response of the GaAs-based BIB detector can extend to $\sim 400 \mu\text{m}$ (1). The effects of different dopants, device structures and host materials on the performances of BIB detectors have been widely studied. However, the systematic investigation on the numerical simulation of the fabrication process, especially of ion implantation and annealing, was seldom reported.

II. DEVICE STRUCTURE AND FABRICATION

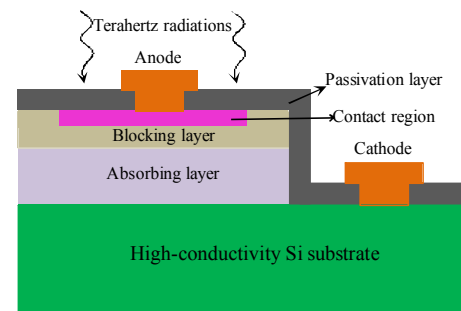


Fig. 1. Structural model of front-illuminated Si-based BIB detector.

The cross-sectional structure of front-illuminated Si-based BIB detector is shown in Fig. 1. It is sequentially composed of a $500\text{-}\mu\text{m}$ -thick high-conductivity Si substrate, a $30\text{-}\mu\text{m}$ -thick Si:P absorbing layer, a $10\text{-}\mu\text{m}$ -thick high-purity Si blocking layer, a 100-nm -thick contact layer formed by P ion implantation and a 200-nm -thick SiO_2 passivation layer. Additionally, The anode and cathode formed with metal films of Ti/Al/Ni/Au were deposited upon the contact layer and the high-conductivity Si substrate, respectively.

*Corresponding author: Juncheng Cao

This work was sponsored by Shanghai Rising-Star Program (Grant No. 17QB1403900), Young Elite Scientists Sponsorship Program by CAST (Grant No. 2018QNR001), the National Natural Science Foundation of China (Grant Nos. 61404120, and 61705201), Shanghai Sailing Program (Grant No. 17YF1418100), and Shanghai Youth Top-Notch Talent Development Program..

The fabrication process flow of the Si-based BIB detector is as follows: Firstly, the Si:P absorbing layer and intrinsic Si blocking layer were both grown by metal organic chemical vapor deposition (MOCVD). Secondly, the contact region was made by P ion implantation and rapid thermal annealing. Thirdly, SiO₂ deposition and mesa etching were completed by plasma enhanced chemical vapor deposition (PECVD) and inductively coupled plasma (ICP) etching, respectively. Finally, anode and cathode were formed by lithography and electron beam evaporation simultaneously.

III. RESULTS AND DISCUSSION

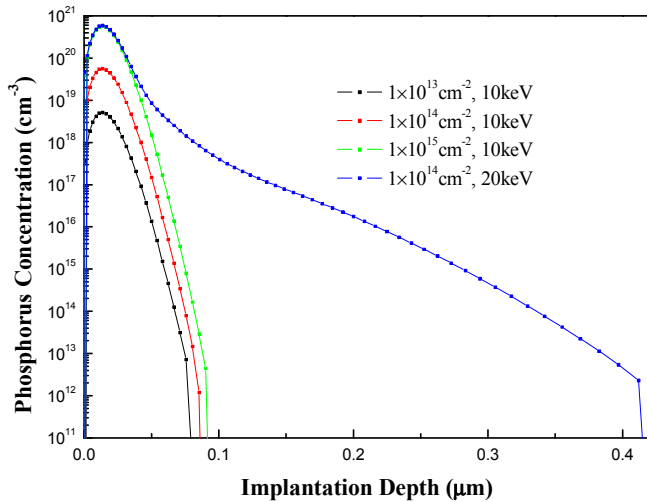


Fig. 2. Doping profiles of P ion implantation with different doses and energies in the contact region. The implantation doses and energies are as follows: $1 \times 10^{13} \text{ cm}^{-2}$ at 10 keV, $1 \times 10^{14} \text{ cm}^{-2}$ at 10 keV, $1 \times 10^{15} \text{ cm}^{-2}$ at 10 keV, $1 \times 10^{14} \text{ cm}^{-2}$ at 20 keV.

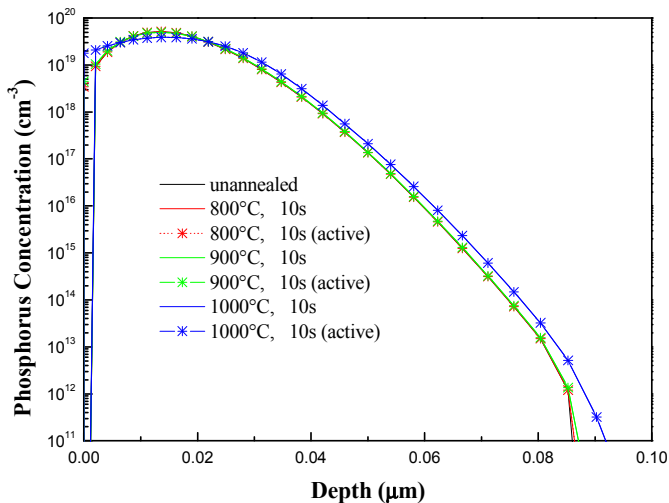


Fig. 3. Concentration distribution of doped Phosphorus and activated Phosphorus under different annealing conditions. The rapid thermal annealing conditions are as follows: unannealed, 10s at 800°C, 10s at 900°C, 10s at 1000°C.

Fig. 2 shows that the depth of P ion implantation is below 100nm at the implantation energy of 10 keV, while the depth

exceeds 400 nm at 20 keV. When the implantation doses are $1 \times 10^{13} \text{ cm}^{-2}$, $1 \times 10^{14} \text{ cm}^{-2}$, and $1 \times 10^{15} \text{ cm}^{-2}$, the dopant concentrations can reach up to $5 \times 10^{18} \text{ cm}^{-3}$, $5 \times 10^{19} \text{ cm}^{-3}$ and $5 \times 10^{20} \text{ cm}^{-3}$, respectively. In principle, the contact region should be not only highly doped ($>10^{19} \text{ at/cm}^3$) to be conductive, but also, thin enough ($<150\text{nm}$) so that its absorption of IR and THz radiations can be neglected. Therefore, the implantation energy of 10keV and the implantation dose of $1 \times 10^{14} \text{ cm}^{-2}$ were selected for the P ion implantation process. Fig. indicates the concentration distributions of Phosphorus and activated Phosphorus are almost the same at every single annealing temperature. The activation rate of P dopant is nearly 100%. The redistribution of P dopant doesn't occur during annealing at 800°C or 900°C. However, obvious redistribution is observed after the annealing of 1000°C, which will deteriorate the detector performance. The 900°C and 10s annealing process was employed to form ohmic contact. Finally, the test results showed that the Si-based BIB detector we fabricated had excellent performances of 10 A/W peak responsivity and 5 ~ 45 μm response spectral range.

IV. CONCLUSION

In this work, a constructed structural model and the fabrication process of Si-based BIB detector were proposed. The P ion implantation and rapid thermal annealing processes for Si-based BIB detector have been optimized by numerical simulation. The simulation results indicate that by 10keV implantation energy and $1 \times 10^{14} \text{ cm}^{-2}$ dose, the high-quality contact region can be achieved, and the 900°C and 10s annealing process is an appropriate approach to activate dopants and form ohmic contact. It is demonstrated that our simulation results provide valuable parameters to improve the performances of Si-based BIB detector.

REFERENCES

- [1] X. D. Wang, B. B. Wang, Y. L. Chen, L. W. Hou, W. Xie, X. Y. Chen, and M. Pan, "Spectral response characteristics of novel ion-implanted planar GaAs blocked-impurity-band detectors in the terahertz domain" *Opt. Quantum Electron.*, Vol. 48, pp. 518-1-12, November 2016.
- [2] W. D. Hu, X. S. Chen, F. Yin, Z. J. Quan, Z. H. Ye, X. N. Hu, Z. F. Li, and W. Lu, "Analysis of temperature dependence of dark current mechanisms for long-wavelength HgCdTe photovoltaic infrared detectors," *J. Appl. Phys.*, Vol. 105, pp. 104502-1-8, June 2009.
- [3] Stephan M. Birkmanna, Jutta Stegmaie, Ulrich Grozinger, et al. "Cold performance tests of blocked-impurity-band Si:As detectors developed for Darwin," *Proc. of SPIE Vol. 7021*, pp. 70210R-1, June 2008.
- [4] James E. Huffman, A. G. Crouse, B. L. Halleck, and T. V. Downes, "Si:Sb blocked impurity band detectors for infrared astronomy," *J. Appl. Phys.*, Vol. 72, pp. 273-275, July 1992.
- [5] S. B. Stetson, D. B. Reynolds, M. G. Stapelbroek and R. L. Stermer, "Design and performance of blocked-impurity-band detector focal plane arrays," *Proc. of SPIE Vol. 686*, pp. 48-60, August 1986.
- [6] Jeffrey W. Beeman, Supriya Goyal, Lothar A. Reichertz and, Eugene E. Haller, "Ion-implanted Ge:B far-infrared blocked-impurity-band detectors," *Infrared Physics & Technology*, vol. 51, 2007, pp. 60-65, March 2007.
- [7] Dan M. Watson, Matthew T. Guptill, James E. Huffman, Timothy N. Krabach, S. Nicholas Raines, and Shobita Satyapal, "Germanium blocked-impurity-band detector arrays: Unpassivated devices with bulk substrates," *J. Appl. Phys.*, Vol. 74, pp. 4199-4205, September 1993.